Computers in Biology and Medicine 43 (2013) 1833–1852

Contents lists available at ScienceDirect

Computers in Biology and Medicine

journal homepage: www.elsevier.com/locate/cbm

Fluid mechanics based classification of the respiratory efficiency of several nasal cavities

Andreas Lintermann*, Matthias Meinke, Wolfgang Schröder

Institute of Aerodynamics, RWTH Aachen University, Wüllnerstr. 5a, 52062 Aachen, Germany

ARTICLE INFO

Article history:
Received 10 June 2013
Accepted 4 September 2013

Keywords:
Lattice Boltzmann
Thermal Lattice Boltzmann
Respiration capability
Heating capability
Nasal cavity flows

ABSTRACT

The flow in the human nasal cavity is of great importance to understand rhinologic pathologies like impaired respiration or heating capabilities, a diminished sense of taste and smell, and the presence of dry mucous membranes. To numerically analyze this flow problem a highly efficient and scalable *Thermal Lattice-BGK (TLBGK)* solver is used, which is very well suited for flows in intricate geometries. The generation of the computational mesh is completely automatic and highly parallelized such that it can be executed efficiently on *High Performance Computers* (*HPCs*). An evaluation of the functionality of nasal cavities is based on an analysis of pressure drop, secondary flow structures, wall-shear stress distributions, and temperature variations from the nostrils to the pharynx. The results of the flow fields of three completely different nasal cavities allow their classification into ability groups and support the *a priori* decision process on surgical interventions.

1. Introduction

The functionality of the human nasal cavity is crucial for the comfort of the individual person, since it not only plays a role in olfaction and degustation, but it also filters the air from particles and moisturizes and heats it to achieve optimal fluid conditions in the lung. As a consequence, a reduction of these functions causes subjective pathological complaints by the individual patient. Functional degradations are not only generated by simple coryza or allergic reactions, but can also occur due to malformations or deformations of the geometric shape of the nasal cavity and as such reduce the inspiration and heating capabilities. In some cases surgical interventions are required to reestablish certain functionalities by geometric optimization of the human nasal cavity. Surgery planning is a challenging task in rhinology and is usually performed based on expert knowledge. To support this decision process, the flow characteristics in the nasal cavity can be numerically analyzed in detail. This development has led to the field of *Computer Assisted Surgery* [1], which allows to better understand the intricate flow physics in a human nasal cavity.

First experimental investigations based on a model of the nasal cavity were performed by Masing [2] and later on complemented by Brücker and Park [3] by measuring the spatial velocity distribution. Highly resolved numerical simulations in the same model of the nasal cavity as that in [3] were conducted by Hörschler et al. [4,5] using an *Advection Upstream Splitting Method* (*AUSM*)-based *Finite-Volume Method* (*FVM*) of second-order accuracy on a multi-block structured grid. Recent simulations with commercial flow solvers were presented in [6–10]. Naftali et al. [6] and Elad et al. [7] use *FLUENT* to simulate the unsteady pulsatile three-dimensional inspiratory flow in a nose-like and in an anatomical model obtained from medical images. Assuming laminar flow they investigate the air-conditioning capacity [6] and the influence of wall-shear stress [7] during inhalation. The results in [6] show that the models can provide up to 90% of the heat flux and moisturization required to achieve sufficient breathing conditions and that the endonasal structural components play a major role in this process. From the investigations by Elad et al. [7] it is known that the wall-shear stress in the simulations reaches values on the order of 1 Pa and that locally even higher stresses can occur, which could effect the functional performance of endothelial and epithelial cells [11,12]. Zachow et al. assumed turbulent flow [8] and use *ANSYS CFX* with an element-based FVM and the *Shear-Stress Transport* (*SST*) turbulence model [13] for the *Reynolds-averaged Navier–Stokes (RANS)* equations to predict the flow in a nasal cavity extracted from *Computer Tomography* (*CT*) images. This study delivers a proof of concept without discussing the respiration and heating capability in detail. Riazuddin et al. [10] used *FLUENT* to solve the *RANS*-equations closed by the *SST* turbulence model for a nasal cavity. Under a variation of the Reynolds number, the velocity, the resistance, the wall-shear stress, vortex formations, and turbulence intensities were investigated for the in- and expiration phase. The results of this study show that the resistance is greater in the inspiratory phase than in the expiratory phase, where the mixing due to turbulence is higher. Hörschler et al. [14] addressed the question of laminar or turbulent flow and

* Corresponding author. Tel.: +49 241 80 90419; fax: +49 241 80 92257.
E-mail addresses: A.Lintermann@aia.rwth-aachen.de (A. Lintermann), M.Meinke@aia.rwth-aachen.de (M. Meinke), office@aia.rwth-aachen.de (W. Schröder).

0010-4825/$ - see front matter © 2013 Elsevier Ltd. All rights reserved.
http://dx.doi.org/10.1016/j.compbiomed.2013.09.003

performed a highly resolved simulation of the flow through a model of the human nasal cavity without incorporating any kind of turbulence model and obtained a good agreement with experimental findings for the primary flow structures. That is the nasal cavity flow which is spatially and temporally in a transitional state could be well described by a sufficient resolution without influencing the numerical solution by turbulence modeling.

The aforementioned investigations focused on model-like geometries or single real nose configurations. They do lack the comparison of the air-conditioning functionality and wall-shear stress distribution for a variety of anatomically correct nasal cavities and hence, can be considered individual solutions. An overview on methods and challenges in nasal cavity flows is presented in Kim et al. [15] in which a short summary on studies investigating septum deviations, turbinectomy, and maxilliary sinus ventilation with respect to nasal resistance, flow allocation, wall-shear stress, heat flux, and humidification are presented. A more detailed investigation on respiration conditions in pre- and post-surgical states and in virtually modified geometries is given in [16,17] where *FLUENT* is used to simulate a steady inspiration. Garcia et al. [16] apply steady-state mass-flux boundary conditions at the nostrils. This generates the same mass-flux in both nasal cavities, which does not correspond to realistic respiration that is determined by the geometry of the left and right cavities. Rhee et al. [17] used approximately 4×10^6 cells, while Garcia et al. [16] used approximately 10^6 cells to resolve the nasal cavity. Yu et al. [9] simulate unsteady in- and expiratory flows for 24 three-dimensional models obtained from medical images, three solutions of which are discussed in great detail. They use *ANSYS* to solve the *RANS*-equations and determine the pressure drop and the volume flux depending on the pressure gradient. The simulations are based on a fully turbulent flow assumption, whereas the flow in the nasal cavity is mostly in the laminar or transitional regime [14,18]. Nevertheless, it is fair to state that *RANS*-based simulations seem to provide reasonable integral results only under certain conditions since turbulence models were developed for different flow regimes. However, nasal cavities are individually different and based on the geometrical configuration unsteady multiscale flow structures can appear that might not be completely captured by the given resolutions. That is regarding the intricacy of human nasal cavities and a detailed analysis of the resulting flow structure either a higher fidelity turbulence model for *RANS*-calculations that represents the local variance of the flow structure is necessary or a higher resolved direct-numerical-simulation-like approach is to be used to capture the time-dependent flow physics inside the nasal cavity.

Therefore, following the findings of Hörschler et al. [14] highly resolved numerical simulations using a *Lattice-Boltzmann Method* (*LBM*) are performed in this investigation. Furthermore, the volume flux will be in a range such that the Reynolds number Re which is proportional to the volume flux will be approximately $Re\approx1900$ and only inspiratory flow will be analyzed, i.e., the transition phase from inspiration to expiration or *vice versa* will not be considered. Hence, considering the results discussed in detail in [5] only steady inhalation will be computed since in the Reynolds number range of $Re\approx1900$ unsteady effects can be neglected on an integral scale. Unlike in former studies [5–8,10,14,18] the flow structures of three completely different nasal cavities are investigated and a classification of the respiratory efficiency based on the flow and the temperature fields is suggested.

This paper is organized as follows. The numerical method, the boundary conditions, the grid generation process, and the quantities to analyze the flow in the nasal cavity are discussed in Section 2. In Section 3 the three different nasal cavities are presented and subsequently, the flow fields of the varying configurations are juxtaposed. That is the pressure drop, the overall three-dimensional flow characteristics, the wall-shear stress, and the heat transfer are analyzed. Based on an evaluation of the various distributions a tentative classification of the respiratory efficiency is given. Finally, some conclusions are drawn in Section 4.

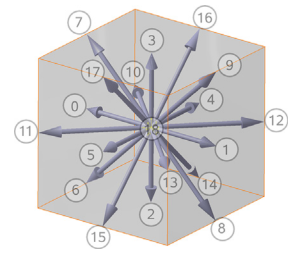

$$\xi_i=\xi_0\begin{cases}(\mp1,0,0)\,;(0,\mp1,0)\,;(0,0,\mp1) & \alpha=0\ldots5\\(\mp1,\mp1,0)\,;(\mp1,0,\mp1)\,;(0,\mp1,\mp1) & \alpha=6\ldots17\\(0,0,0) & \alpha=18\end{cases}$$

Fig. 1. D3Q19 model for phase space discretization. In three dimensions 19 directions are specified to model molecular collision and propagation processes.

Table 1
Computation of macroscopic variables from moments of the PPDFs.

Variable	*Discrete moment*
Density	$\rho=\sum_{i=0}^{18}f_i=\sum_{i=0}^{18}f_i^{eq}$
Momentum	$\rho v_\alpha=\sum_{i=0}^{18}\xi_{i,\alpha}f_i=\sum_{i=0}^{18}\xi_{i,\alpha}f_i^{eq}$
Temperature	$T=\sum_{i=0}^{18}g_i=\sum_{i=0}^{18}g_i^{eq}$

2. Numerical method

To simulate the flow in the nasal cavity a *Lattice-Boltzmann Method* (*LBM*) is used since it is well known that such an approach has some major advantages over *Finite-Element* (*FE*) or *Finite-Volume* (*FV*) methods when highly intricate geometries are considered [19]. Among other applications [20] the *LB* method has been proven to be well suited for bio-mechanical flow problems in the moderate Reynolds number regime, i.e., for flow simulations in the human lower respiratory system [21,22]. In addition, a good parallel scale-up and straightforward boundary treatment makes the *LB* method attractive to simulate nasal cavity flows as it has been shown by Finck et al. [18] and Eitel et al. [23]. The *LB* code used in this study has been previously used and validated by Freitas and Schröder [21] and Eitel-Amor et al. [20]. In the following, a brief description of the *LB* method is given, the mesh generation process is described, and the numerical approaches to analyze and categorize nasal cavity flows are presented.

2.1. Governing equations and notations

The *Lattice-Boltzmann Method* is a gas-kinetic stochastical approach to simulate continuum flows by numerically solving the *Boltzmann equation*, i.e., by solving for the particle probability density functions f_i (PPDFs) in the *Lattice-Bhatnagar–Gross–Krook equation* [24]

$$f_i(\vec{x}+\xi_i\delta t,t+\delta t)=f_i(\vec{x},t)+\omega\delta t\cdot(f_i^{eq}(\vec{x},t)-f_i(\vec{x},t)) \quad (1)$$

in three dimensions with the D3Q19 model [25] shown in Fig. 1. To determine the temperature field a multi-distribution function approach (MDF) described in [26–29] is used, where in addition to